Received: 14 December 2019 | Revised: 16 April 2020 | Accepted: 22 April 2020

DOI: 10.1002/ardp.201900368

Check for updates

FULL PAPER

DPhG ARCH PHARM Archiv der Pharmazie

2-Aminoaryl-3,5-diaryl pyrazines: Synthesis, biological evaluation against *Mycobacterium tuberculosis* and docking studies

Nagaraja Reddy Gangarapu[1,2] | Archakam Ranganatham[3] | Eeda Koti Reddy[4] | Shivaraj Yellappa[1] | Kothapalli Bannoth Chandrasekhar[2]

[1]Department of Chemistry, Bangalore University, Bengaluru, Karnataka, India

[2]Department of Chemistry, Jawaharlal Nehru Technological University, Ananthapuramu, Andhra Pradesh, India

[3]Laboratory Division, National Tuberculosis Institute, Bangalore, Karnataka, India

[4]Department of Science and Humanities, Division of Chemistry, Vignan's Foundation for Science, Technology and Research-VFSTR (Deemed to be University), Guntur, Andhra Pradesh, India

Correspondence
Shivaraj Yellappa, Department of Chemistry, Bangalore University, Jnanabharathi Campus, Bengaluru, Karnataka 560056, India.
Email: shivaraj_y@rediffmail.com

Abstract

Rationally designed *Mycobacterium tuberculosis* (Mtb) inhibitors were synthesized under Buchwald conditions using $Pd_2(dba)_3$/xantphos and the compounds were investigated for their biological activity against the Mtb standard strain H37Rv and two other clinically isolated multidrug-resistant strains with different drug resistance patterns. Compounds **5e**, **6e**, **7e**, and **8e** exhibited excellent antituberculosis activity against H37Rv with a minimum inhibitory concentration (MIC) value of 15 μg/ml. Compounds **5a**, **6c**, **7b**, **8a**, **8b**, and **8d** also displayed their potency with a MIC value in the range of 15–25 μg/ml. In addition to the Mtb studies, compounds **4e**, **5e**, **7e**, and **8e** were tested for cytotoxicity on HEK-293 cells and compounds **7e** and **8e** were identified to have low toxicities of up to 200 and 300 μM, respectively. The synthesized compounds docked with the 2FUM protein of Mtb and the docking studies revealed that compounds **5e**, **6e**, **7e**, and **8e** can bind strongly in the active site of the enzyme and showed binding energies of −9.62, −10.7, −11.48, and −12.06 kcal/mol, respectively. Compound **7e** forms four hydrogen bonds, whereas compound **8e** forms five hydrogen bonds with amino acids, respectively. Based on these results, compounds **7e** and **8e** might be considered potential lead compounds with good anti-Mtb potency.

KEYWORDS

antituberculosis activity, cytotoxic activity, synthesis

1 | INTRODUCTION

Tuberculosis (TB) is the most conspicuous disease among all pathogenic diseases. Globally, more than two million lives are lost every year due to TB and about 11 million new patients have been identified.[1] The medicine for tuberculosis is insufficient to address the many challenges of treatment, whereas the tuberculosis patients were decreased by an average of 1.5% every year. The aim of the World Health Organization (WHO) is to eradicate this infectious disease by 90% and loss of lives by 95%.[2] The treatment of TB is very complicated and more awareness needs to be raised among the individuals. Tuberculosis is still a major disease worldwide, the incidence of which continues to increase in developing countries.[3] Even though medical treatment is currently available to cure tuberculosis, there are some disadvantages such as the timeline for treatment, the need to focus on multidrug therapy, and the emergence of drug resistance, HIV coinfection, and persistence of *Mycobacterium tuberculosis* (Mtb) bacilli.[4,5] The process of multidrug medical treatment takes 6 months, consisting of isoniazid (INH), rifampicin (RMP), pyrazinamide (PZA), and ethambutol (EMB) for 2 months, followed by fully susceptible isolates of RMP and INH for 4 months.[6–8] A key question is how

 © 2020 Deutsche Pharmazeutische Gesellschaft

robust our approaches are toward the discovery of new TB drugs, and the measures that could be taken to reduce the length of protracted clinical development of new drugs. Several derivatives with antitubercular activity have been described such as benzimidazole ureas (**1**)[9] from Vertex Pharma, PZA derivatives[10] (**2**) from AstraZeneca Pharma, quinoline derivatives from GSK Pharma,[11] and the nitrobenzothiazinone derivative (BTZ043),[12] and azaindole derivatives[13] (Figure 1) of known molecules have been reported as promising drug candidates in preliminary studies. New strategies have to be developed for tuberculosis disease by screening libraries of small molecules for biologically active molecules. Nowadays, treatment with bedaquiline and PA-824 is the new antitubercular regime for chemotherapy. Bedaquiline[14] is a new drug for anti-TB, which was approved by the WHO in 2012, and used in combination with other TB drugs to treat pulmonary TB in adults having multidrug-resistant TB (MDR-TB). However, bedaquiline is a highly lipophilic drug (logP 7.25) with a tendency to cause liver toxicity. Bedaquiline-containing treatments are more cost effective compared with injectable-containing treatments. As part of research to develop new molecules for anti-TB, our team developed a series of 3,5-disubstituted 2-aminopyrazine derivatives and evaluated their anti-TB activity.[15] 2-Aminopyrazine derivatives have biological importance because of their anticancer,[16] CHK1 inhibitor,[17] *Trypanosoma brucei* inhibitor,[18] antimalarial,[19] GSK3β inhibitor,[20] PDK inhibitor,[21] and anticonvulsant activities. To extend our research,[22] we synthesized novel 3,5-disubstituted 2-aminopyrazine derivatives and evaluated their antimycobacterial activity. The binding nature, physicochemical properties (ADME), and cytotoxicity studies for synthesized compounds were also analyzed.

2 | RESULTS AND DISCUSSION

2.1 | Synthetic studies

The synthesis of 2-aminoaryl 3,5-disubstituted pyrazine molecules[23] is shown in Schemes 1 and 2. The compound 3,5-dibromo-2-aminopyrazine (**2**) was synthesized from the reaction of 2-aminopyrazine (**1**) by treatment with bromosuccinimide in dimethyl sulfoxide (DMSO) and Na_2CO_3 as a base for 12 hr at room temperature to yield 3,5-dibromo-2-aminopyrazine (**2**). The intermediate **2** was subjected to Suzuki–Miyaura cross-coupling reaction with different boronic acids (**3**) to obtain compound **4**. The *N*-arylation of compound **4** was screened using different palladium catalysts such as $Pd(OAc)_2$/BINAP, $Pd(OAc)_2$/Xphos, $Pd(OAc)_2$/t-BuXphos, $Pd(OAc)_2$/xantphos, and $Pd_2(dba)_3$/xantphos with different bases like *t*-BuOK, *t*-BuONa, Na_2CO_3, Cs_2CO_3, $K_3PO_4{\cdot}3H_2O$, and K_2CO_3, and different solvents like 1,4-dioxane, toluene, dimethylformamide (DMF), dimethylacetal (DMA), and dimethoxyethane (DME). Among all the screened conditions, compounds **5**–**8** synthesized using $Pd_2(dba)_3$/xantphos and Cs_2CO_3 as a base in DMA at 120°C under microwave irradiation for 2 hr gave a good yield (70–85%; Table 1).

2.2 | Docking results

In this study, FUM protein was used as a standard and it plays a vital role in the growth inhibition of mycobacteria. Fumarase (Fum) is an enzyme of the canonical tricarboxylic acid cycle and is dispensable in many organisms. Transposon mutagenesis studies in Mtb, however,

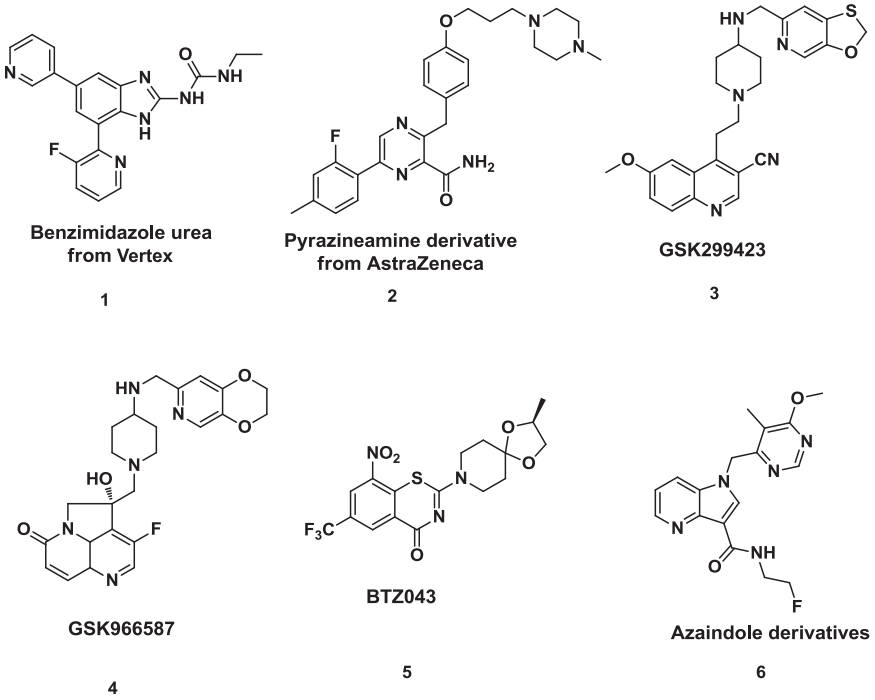

FIGURE 1 Biologically active antituberculosis molecules

SCHEME 1 Synthesis of 2-aminoaryl-3,5-disubstituted pyrazines

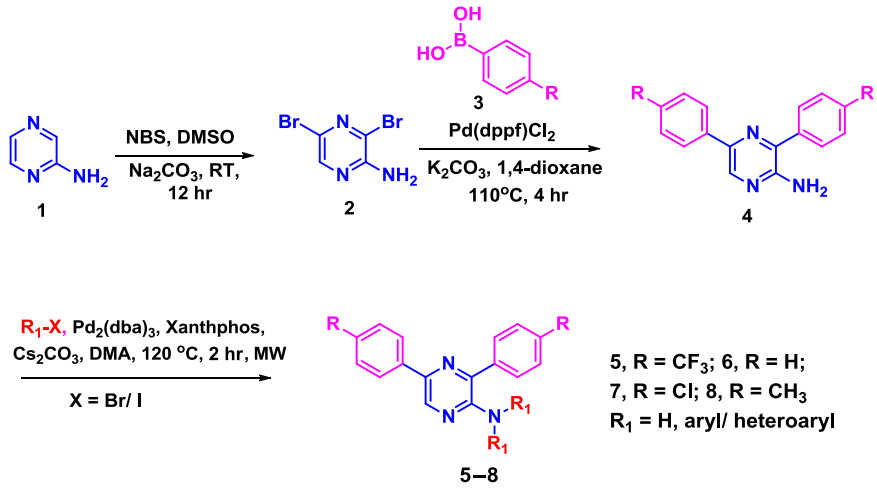

indicate that Fum is required for optimal growth. Here, the generation and characterization of a genetically engineered Mtb strain in which Fum expression is conditionally regulated are reported. These results identify Mtb Fum as a potentially species-specific drug target whose inactivation may kill Mtb through a covalently irreversible form of metabolic toxicity. The intention behind the selected FUM protein to prove the derivative showed good anti-TB activity as well as anticancer agent which will be expedited in further, the mechanism of PZA was explained in detail.

Accordingly, the synthesized compounds were subjected to in silico docking studies with the tuberculosis protein (Figures 2–4). These studies show various kinds of interactions such as hydrogen bonding, electrostatic interaction, and van der Waals bonding. All the compounds have binding energies ranging between −12.06 and −6.7 kcal/mol. However, among the synthesized compounds, **8e** presented excellent interaction with the protein and strong binding energy of −12.06 kcal/mol. Compound **8e** showed an inhibitory concentration of 7.88 μM with five hydrogen bonds. The hydrogen bond interaction within the active site of amino acids VAL95, GLY59, ASP156, PHE19, and LEU17 in the protein sequence. Correspondingly, compounds **5e**, **6e**, and **7e** displayed strong binding interaction with the protein with binding energies of −9.62, −10.7, and −11.48 kcal/mol, respectively. These derivatives exhibited inhibitory concentrations of 88.1, 14.41, and 3.87 μM, respectively. Compounds **6e** and **7e** exhibited four hydrogen bonding interactions within the active site of amino acids ASP156, GLU59, LEU17, and VAL95. However, compounds **3a**, **4a**, **5a**, and **6a** displayed strong binding interaction with the protein with binding energies of −8.17, −9.15, −8.74, and −8.85 kcal/mol, respectively (Table 2). The remaining synthesized molecules have shown moderate to good binding energy interactions. Moreover, the reference drug RMP displays three strong H-bond interactions within the active site of amino acids VAL95, PHE19, and ASP156 with a binding energy of −9.16 kcal/mol. Other standard drugs such as PZA and INH showed good binding energies of −4.29 and 3.16 kcal/mol with three and one H-bond interaction with different amino acids and inhibitory concentrations of 711.2 and 4.85 μM, respectively.

2.3 | Results of biological activity

This study aims to discuss pyrazine derivatives and their activity against Mtb and other drug-resistant mycobacterial strains. The experimental process for testing anti-TB drug susceptibility was based on the H37Rv tuberculosis standard strain and another two clinically isolated multidrug-resistant strains with different drug-resistant patterns; the minimum inhibitory concentration (MIC) experiment was carried out using different drug concentrations on the Lowenstein–Jensen (LJ) medium.

The experimental results of antimycobacterial activity are shown in Table 3. It shows that all the tested compounds showed good biological activity in the used test strains of Mtb. All the compounds, in particular, were found to be effective against mycobacteria at a concentration ranging from 4.0 to 40 μg/ml in drug-containing LJ medium. RMP and INH, used as positive drug controls, at concentrations of about 40 and 0.2 μg/ml, respectively, were prepared as per the standard guidelines of drug susceptibility testing (DST) by the Revised National Tuberculosis Control Program (RNTCP), Government of India, at the National Tuberculosis Institute (NTI), Bangalore. The bioactivities of the derivatives were assayed using a MIC experiment. All the synthesized compounds showed good inhibition range from 15 to 50 μg/ml. In the structure–activity relationship (SAR) studies, the compounds with a dipyridyl substitution at the amino group such as **5e**, **6e**, **7e**, and **8e** displayed a very good MIC value of 15 μg/ml. Similarly, the compounds with a monopyridyl substitution on the amine group such as **7b** and **8b** exhibited moderate to good MIC values of 15 and 25 μg/ml, respectively. The other pyridyl substitution derivatives such as **5b** and **6b** showed good MIC values in the range of 25–50 μg/ml. The compound with 6-chloropyrimidine substitution on amino group (**6c**) presented a

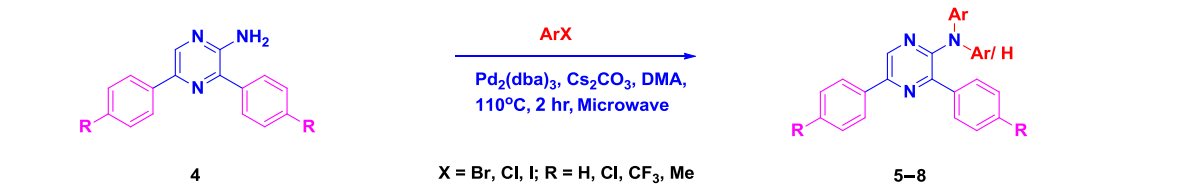

4 X = Br, Cl, I; R = H, Cl, CF_3, Me 5–8

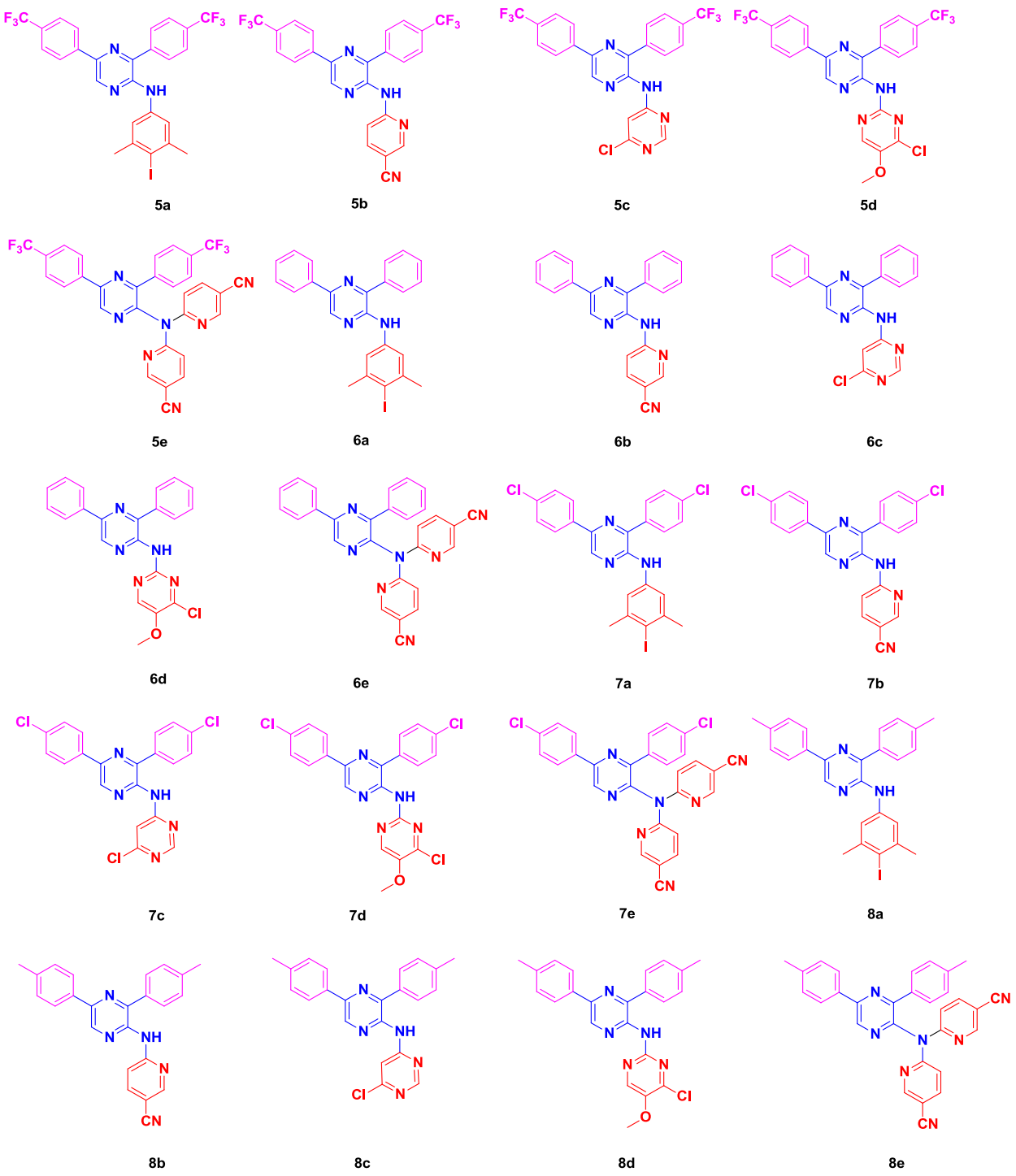

SCHEME 2 Substrate scope of the 2-aminoaryl-3,5-disubstituted pyrazines

TABLE 1 Optimization for the synthesis of compounds **5–8**

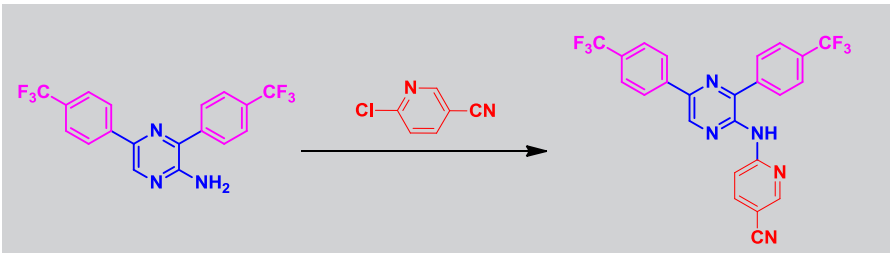

Sl. No.	Catalyst (0.1 equiv)/ligand (0.2 equiv)	Base (2.0 equiv)	Solvent	Temp (°C)	% of yield
1	$Pd_2(OAc)_2$	Na_2CO_3	1,4-Dioxane	110	NA
2	$Pd_2(OAc)_2$/Xphos	Na_2CO_3	1,4-Dioxane	110	10
3	$Pd_2(OAc)_2$/t-BuXphos	Na_2CO_3	1,4-Dioxane	110	13
4	$Pd_2(OAc)_2$/xantphos	Na_2CO_3	1,4-Dioxane	110	20
5	$Pd_2(OAc)_2$/xantphos	K_2CO_3	1,4-Dioxane	110	25
6	$Pd_2(OAc)_2$/xantphos	Cs_2CO_3	1,4-Dioxane	110	50
7	$Pd_2(OAc)_2$/xantphos	*t*-BuOK	1,4-Dioxane	110	34
8	$Pd_2(OAc)_2$/xantphos	$K_3PO_4{\cdot}3H_2O$	1,4-Dioxane	110	35
9	$Pd_2(dba)_3$/xantphos	Cs_2CO_3	1,4-Dioxane	110	57
10	$Pd_2(dba)_3$/xantphos	Cs_2CO_3	Toluene	110	20
11	$Pd_2(dba)_3$/xantphos	Cs_2CO_3	DMF	110	62
12	$Pd_2(dba)_3$/xantphos	Cs_2CO_3	DMA	110	78
13	$Pd_2(dba)_3$/xantphos	Cs_2CO_3	DMA	120	85
14	$Pd_2(dba)_3$/xantphos	Cs_2CO_3	DME	120	50

Note: All reactions were carried out under microwave heating.
Abbreviations: DMA, dimethylacetal; DME, dimethoxyethane; DMF, dimethylformamide.

very good inhibitory value of 15 μg/ml. The other pyrimidine substitution derivatives **5c**, **7c**, and **8c** showed good MIC values in the range of 25–50 μg/ml. The compounds with the substitution of 4-iodo-3,5-dimethylphenyl derivatives (**5a**, **6a**, **7a**, and **8a**) also exhibit good MIC values in the range of 15–50 μg/ml. The other compounds were also ideal with MIC values in the range of 25–50 μg/ml. SAR studies revealed that the compounds bearing a dipyridyl group on the amine group could potentially become drug candidates for TB and further studies of clinical trials and in vivo experiments will be initiated in future.

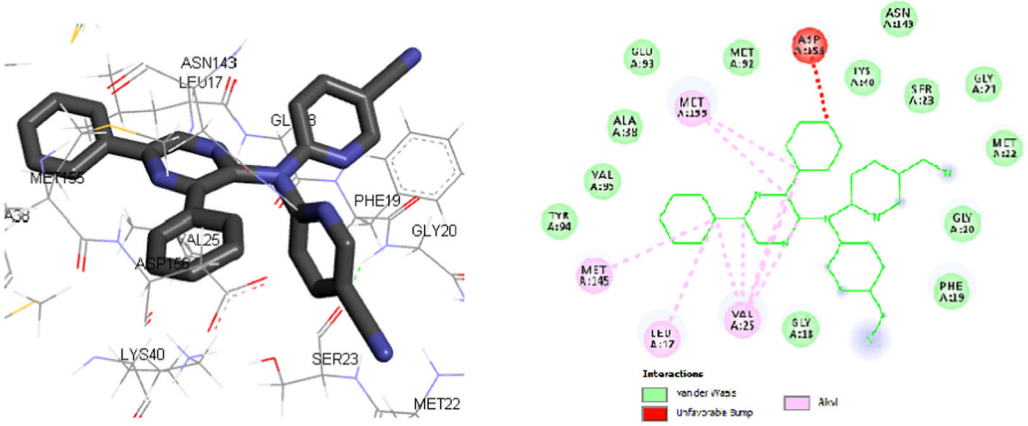

FIGURE 2 Binding interactions, van der Waals interactions, and covalent hydrogen bond interactions in compound **6e**

2.4 | DST results

Selection of control strains of Mtb and its DST pattern with the standard anti-TB drugs (positive controls) used in the RNTC Program. Three strains were used to test the anti-TB activity based on different drug-resistant patterns. All these cultures were collected from the culture bank of NTI and the standard DST results were obtained through NTI laboratory. In addition, standard DST results were obtained through RNTCP guidelines, which were used as comparative standards for this study.

2.5 | Cytotoxicity studies

The in vitro cytotoxicities of most potent antitubercular analogues (**5e**, **6e**, **7e**, and **8e**) were tested in human embryonic kidney cells (HEK-293) by the MTT (3-(4,5-dimethylthiazol-2-yl)-2,5-diphenyltetrazolium bromide) assay method (Figure 5). Its main application is to assess the viability (cell counting) and the proliferation of cells. It can also be used to determine the cytotoxicity of medicinal agents and toxic materials. The compounds were tested using three different concentrations (50, 100, and 200 μM). Compounds **5e** and **6e** displayed toxicity when the concentration was above 100 μM and, for the other molecules, **7e** and **8e** were not toxic up to 200 μM concentration.

2.6 | ADMET results

2.6.1 | In silico predictions of the synthesized compounds

The newly synthesized compounds were evaluated for their drug-like behavior through in silico predictions. The ADMET (absorption, distribution, metabolism, excretion, and toxicity) profiles of the compounds are given in Table 4. Some of the important parameters are molecular weight (MW), partition coefficient (logP), number of hydrogen bond donors and acceptors (HBD and HBA), topological polar surface area (TPSA), number of rotatable groups (rotor), $CaCO_2$ permeability (logPapp; cm/s), Cyp2C19 substrate, Cyp2c19 inhibition, and human intestinal absorption (HIA) were predicted by in silico studies. It was found that the values of MW and logP of all the molecules were within the desired range, except compound **5a**. Number of rotor, HBD, HBA, and TPSA were in the ideal range for all the compounds. The HIA and blood–brain barrier (BBB) of all the compounds was in the preferred range.

3 | CONCLUSION

In this study, we reported the synthesis of 3,5-disubstituted-2-aminoaryl pyrazine molecules with good yields using $Pd_2(dba)_3$/xantphos. The compounds prepared were tested for their anti-tuberculosis activity using H37Rv and with two clinically isolated

	Standard DST results with first-line anti-TB drugs by the 1% proportion method				Standard DST results with second-line anti-TB drugs by the 1% proportion method			
Strain ID	Isoniazid (0.2 μg/ml)	Rifampicin (40 μg/ml)	Ethambutol (2 μg/ml)	Pyrazinamide (100 μg/ml)	Kanamycin (2.5 μg/ml)	Amikacin (1 μg/ml)	Capreomycin (2.5 μg/ml)	Ofloxacin (2 μg/ml)
H37Rv	S	S	S	S	S	S	S	S
Mtb strain 1	R	R	R	R	R	R	R	S
Mtb strain 2	S	S	S	S	R	R	R	R

Abbreviations: DST, drug susceptibility testing; R, resistant; S, sensitive; TB, tuberculosis.

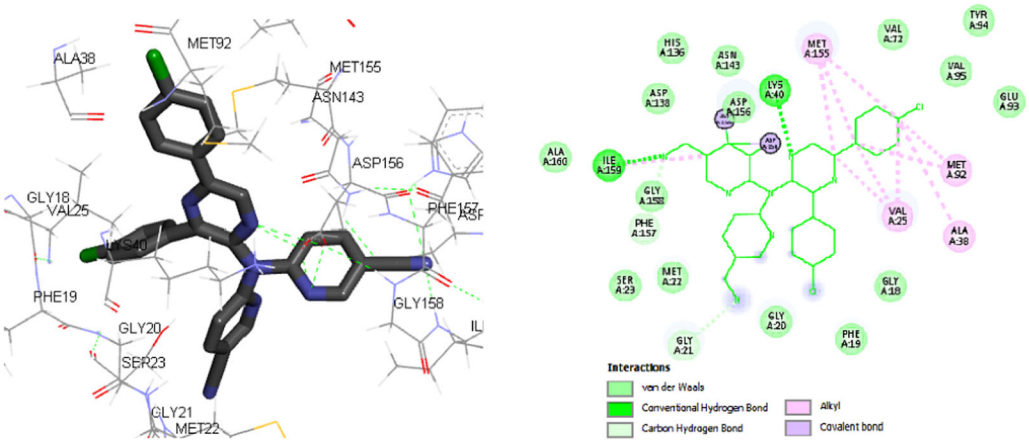

FIGURE 3 Binding interactions, van der Waals interactions, and covalent hydrogen bond interactions in compound **7e**

strains. The motifs with a diaryl substitution of 4-cyano-2-pyridine molecules displayed a very good MIC value of around 15 μg/ml in all three strains. The cytotoxic studies reveal that compounds **5e** and **6e** were nontoxic up to 100 μM and compounds **7e** and **8e** were safe up to 200 μM. The docking studies revealed that compounds **5e**, **6e**, **7e**, and **8e** can bind strongly in the active site of enzyme and showed binding energies of −9.62, −10.7, −11.48, and −12.06 kcal/mol, respectively. Based on our results, compounds **7e** and **8e** might be considered potential lead compounds with good anti-Mtb potency.

4 | EXPERIMENTAL

4.1 | Chemistry

4.1.1 | General

The original nuclear magnetic resonance (NMR) spectra of the investigated compounds are provided as Supporting Information Data, as are their InChI codes together with some biological activity data.

4.1.2 | Experimental procedure for the synthesis of compounds 5a–8e

To a solution of compound **1** (0.130 mmol) in dimethylacetamide as a solvent (5 ml) was added the corresponding aryl/heteroaryl halide **2** (0.393 mmol), followed by the addition of Cs_2CO_3 (0.26 mmol) and $Pd_2(dba)_3$ (0.013 mmol), and the reaction mixture was degassed for 10 min with argon at room temperature. Xantphos (0.026 mmol) was further added and the reaction mixture was heated at 120°C for 2 hr under microwave irradiation. The reaction mixture was quenched with saturated ammonium chloride (20 ml) and extracted with ethyl acetate (2 × 20 ml). The combined organic layers were washed with brine solution (30 ml), dried over anhydrous sodium sulfate, and concentrated under vacuum. The crude was purified by column chromatography using 5–20% of ethyl acetate in hexane and gave compound **5** (70–85%).

*3,5-Bis[4-(trifluoromethyl)phenyl]-*N*-(4-iodo-3,5-dimethylphenyl)-pyrazin-2-amine (**5a**)*

Off-white solid; yield: 60 mg, 75%; melting range: 211–213°C; ^{1}H NMR (500 MHz, $CDCl_3$) δ 8.67 (s, 1H), 8.10–8.08 (d, J = 10.0 Hz, 2H),

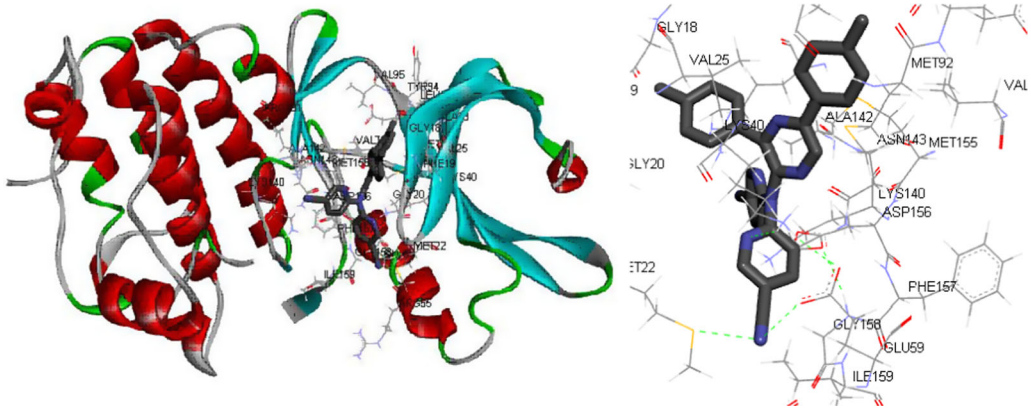

FIGURE 4 Binding interactions in compound **8e**

TABLE 2 The binding energetics of the compounds at the active site of 2FUM

Ligand	H-bonds	Binding energy	IC (μM)	Binding amino acids	Interacting amino acids
5a	0	−8.17	1.03	–	THR179, ALA180, LYS140, ASN143, GLN181, ASP102, THR99, GLY18, MET155, LEU17, PHE19, MET92, ALA38, GLU93, VAL95
5b	1	−7.0	7.37	VAL72	MET92, MET155, ALA63, ASP156, LEU17, PHE19, GLY20, GLY21, ASN143, LYS140, GLN181, THE157, THR179, ALA180
5c	2	−7.5	6.74	VAL95, GLU93	ALA38, VAL72, TYR94, ASP96, GLY97, ARG101, VAL25, MET92, ALA142, THR99, LEU17
5d	0	−6.7	12.18	–	ALA180, GLN181, LYS140, ASN143, ASP156, MET155, ASP102, VAL72, VAL75, GLY97, MET92, LEU17, GLY21, GLY20, PHE19
5e	2	−9.62	88.1	ASP156, LEU17	PHE19, GLY20, GLN181, MET155, ASN143, GLN97, VAL95, THR94, MET92
6a	0	−9.15	197.36	–	PHE19, GLY20, PHE157, VAL25, MET92, LEU17, ALA38, THR94, ASN143, MET155, VAL72, VAL95, GLU93, GLY97
6b	2	−8.03	1.29	VAL95, GLY97	LEU17, ALA38, GLU93, MET92, MET155, PHE19, ASN143, GLY20
6c	0	−7.61	2.65	–	GLY18, PHE19, VAL25
6d	0	−8.16	1.04	–	PHE19, VAL25
6e	4	−10.7	14.41	ASP156, GLU59, VAL95, LEU17	PHE19, GLY18, THR94, ASP96, MET92, ALA38, GLU93, MET155, PHE157, GLY97
7a	0	−8.74	390.2	–	PHE157, GLY20, PHE19, VAL25, MET92, ALA38, GLU93, VAL95, GLY97, ASP102, ASN143, MET155
7b	1	−7.84	1.8	VAL95	PHE19, VAL25, GLY18, LEU17, GLY97, ASP96, THR94, GLY93, ALA35, MET92, VAL74
7c	0	−7.89	1.64	–	GLY18, PHE19, VAL25
7d	0	−7.94	1.52	–	PHE19, VAL25
7e	4	−11.48	3.87	GLU59, ASP156, LEU17, VAL95	PHE19, GLY18, ALA38, PHE157, MET92, VAL72, GLU93, THR94, GLY97, ASP96
8a	0	−8.85	326.24	–	ASP102, GLY97, VAL95, ALA38, GLU39, MET92, PHE157, GLY20, VAL25, ASP143, PHE19, MET155
8b	1	−8.11	1.14	VAL95	PHE19, GLY18, VAL25, LEU17, GLY97, VAL72, GLU93, ALA35, THR94, ASP96, MET92
8c	0	−7.84	1.8	–	VAL25
8d	0	−7.54	2.95	–	PHE19, VAL25
8e	5	−12.06	7.88	GLY59, ASP156, PHE19, VAL95, LEU17	GLY18, PHE157, MET155, VAL72, MET92, GLU93, ASP96, GLY97, TYR94, ALA38
Rifampicin	3	−9.16	672.8	ASP156, PHE19, VAL95,	PHE19, GLY18, VAL25, LEU17, GLY97, VAL72, PHE157
Pyrazinamide	3	−4.29	711.2	TYR75, ASP36, ASP36	ALA64, ARG35, TYR94
Isoniazid	1	3.16	4.85	ARG101	GLY212, GLU213, PRO214, GLY218

Abbreviation: IC, inhibitory concentration.

TABLE 3 Drug susceptibility testing results of tested compounds

Compound ID	Tested Mtb strain	Growth control on plain LJ medium	15 μg/ml	25 μg/ml	50 μg/ml
5a	H37Rv	++	Sensitive	Sensitive	Sensitive
	Mtb strain 1	++	Sensitive	Sensitive	Sensitive
	Mtb strain 2	++	Sensitive	Sensitive	Sensitive
5b	H37Rv	+++	Resistant	Resistant	Sensitive
	Mtb strain 1	++	Resistant	Resistant	Sensitive
	Mtb strain 2	++	Resistant	Resistant	Sensitive
5c	H37Rv	++	Resistant	Resistant	Sensitive
	Mtb strain 1	++	Resistant	Resistant	Sensitive
	Mtb strain 2	++	Resistant	Resistant	Sensitive
5d	H37Rv	+++	Resistant	Resistant	Sensitive
	Mtb strain 1	++	Resistant	Resistant	Sensitive
	Mtb strain 2	++	Resistant	Sensitive	Sensitive
5e	H37Rv	+++	Sensitive	Sensitive	Sensitive
	Mtb strain 1	++	Sensitive	Sensitive	Sensitive
	Mtb strain 2	++	Sensitive	Sensitive	Sensitive
6a	H37Rv	++	Resistant	Sensitive	Sensitive
	Mtb strain 1	++	Resistant	Resistant	Sensitive
	Mtb strain 2	++	Resistant	Sensitive	Sensitive
6b	H37Rv	++	Resistant	Sensitive	Sensitive
	Mtb strain 1	++	Resistant	Resistant	Sensitive
	Mtb strain 2	++	Resistant	Resistant	Sensitive
6c	H37Rv	++	Sensitive	Sensitive	Sensitive
	Mtb strain 1	+++	Sensitive	Sensitive	Sensitive
	Mtb strain 2	+++	Sensitive	Sensitive	Sensitive
6d	H37Rv	++	Resistant	Sensitive	Sensitive
	Mtb strain 1	+++	Resistant	Resistant	Sensitive
	Mtb strain 2	++	Resistant	Resistant	Sensitive
6e	H37Rv	++	Sensitive	Sensitive	Sensitive
	Mtb strain 1	++	Sensitive	Sensitive	Sensitive
	Mtb strain 2	+++	Sensitive	Sensitive	Sensitive
7a	H37Rv	+++	Resistant	Resistant	Sensitive
	Mtb strain 1	++	Resistant	Resistant	Sensitive
	Mtb strain 2	++	Resistant	Resistant	Sensitive
7b	H37Rv	++	Sensitive	Sensitive	Sensitive
	Mtb strain 1	++	Sensitive	Sensitive	Sensitive
	Mtb strain 2	++	Sensitive	Sensitive	Sensitive
7c	H37Rv	++	Resistant	Resistant	Sensitive
	Mtb strain 1	+++	Resistant	Resistant	Sensitive
	Mtb strain 2	++	Resistant	Resistant	Sensitive
7d	H37Rv	++	Resistant	Resistant	Sensitive
	Mtb strain 1	++	Resistant	Resistant	Sensitive
	Mtb strain 2	++	Resistant	Resistant	Sensitive
7e	H37Rv	+++	Sensitive	Sensitive	Sensitive
	Mtb strain 1	++	Sensitive	Sensitive	Sensitive
	Mtb strain 2	++	Sensitive	Sensitive	Sensitive
8a	H37Rv	+++	Sensitive	Sensitive	Sensitive
	Mtb strain 1	++	Sensitive	Sensitive	Sensitive
	Mtb strain 2	++	Sensitive	Sensitive	Sensitive

(Continues)

TABLE 3 (Continued)

Compound ID	Tested Mtb strain	Growth control on plain LJ medium	15 μg/ml	25 μg/ml	50 μg/ml
8b	H37Rv	+++	Resistant	Resistant	Sensitive
	Mtb strain 1	++	Resistant	Sensitive	Sensitive
	Mtb strain 2	+++	Resistant	Resistant	Sensitive
8c	H37Rv	+++	Resistant	Sensitive	Sensitive
	Mtb strain 1	++	Resistant	Resistant	Sensitive
	Mtb strain 2	+++	Resistant	Resistant	Sensitive
8d	H37Rv	+++	Sensitive	Sensitive	Sensitive
	Mtb strain 1	++	Sensitive	Sensitive	Sensitive
	Mtb strain 2	+++	Sensitive	Sensitive	Sensitive
8e	H37Rv	+++	Sensitive	Sensitive	Sensitive
	Mtb strain 1	+++	Sensitive	Sensitive	Sensitive
	Mtb strain 2	++	Sensitive	Sensitive	Sensitive

Note: +++, ++ indicate Confluent growth and >100 colonies respectively.
Abbreviations: LJ, Lowenstein–Jensen; Mtb, *Mycobacterium tuberculosis*.

7.94–7.93 (d, J = 5.0 Hz, 2H), 7.86–7.84 (d, J = 10.0 Hz, 2H), 7.72–7.70 (d, J = 10.0 Hz, 2H), 7.30 (s, 2H), 6.70 (s,1H), 2.47 (s, 6H); ^{13}C NMR (126 MHz, $CDCl_3$) δ 148.42 (s), 142.74 (s), 141.58 (s), 140.08, 140.02, 139.89 (t), 138.41, 138.25 (d), 129.13 (s), 129.48, 129.45 (d), 125.89, 125.86, 125.83 (t), 118.63 (s), 29.73 (s). Ultraperformance liquid chromatography–mass spectrometry (UPLC–MS): *m/z* calculated for $C_{26}H_{18}F_6IN_3$: 613.34; observed mass: 614.8 $[M + H]^+$.

*6-{3,5-Bis[4-(trifluoromethyl)phenyl]pyrazin-2-ylamino}pyridine-3-carbonitrile (**5b**)*

Off-white solid; yield: 51 mg, 80.5%; melting range: 230–232°C; ^{1}H NMR (500 MHz, $CDCl_3$) δ 8.79 (s, 1H), 8.64–8.63 (d, J = 8.5.0 Hz, 1H), 8.50 (d, J = 1.5 Hz,1H), 8.15–8.13 (d, J = 8.0 Hz, 2H), 7.96–7.88 (m, 6H), 7.76–7.74 (d, J = 8.0 Hz, 2H); ^{13}C NMR (126 MHz, $CDCl_3$) δ 154.57 (s), 151.87 (s), 145.96 (s), 144.01 (s), 141.40 (s), 141.27 (s), 139.23 (s), 139.05 (s), 137.78 (s), 129.25 (s), 126.67–126.65 (d), 126.38 (s), 126.02–125.99 (d), 117.18 (s), 112.05 (s), 103.04 (s); UPLC–MS: *m/z* calculated for $C_{24}H_{13}F_6N_5$: 485.38; observed mass: 482.2 $[M + H]^+$.

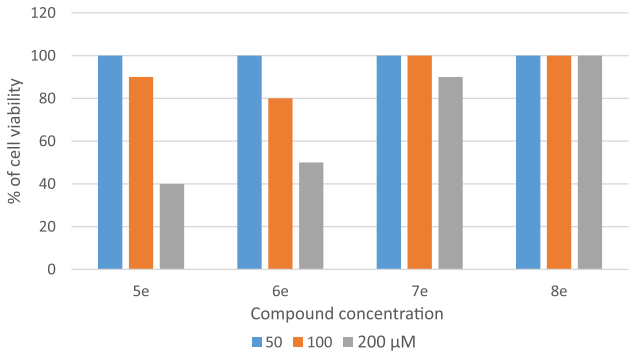

FIGURE 5 Cell viability of more potent compounds on HepG2 cells after 24-hr treatment

*N-{(3,5-Bis[4-(trifluoromethyl)phenyl]pyrazin-2-yl}-6-chloropyrimidin-4-amine (**5c**)*

Off-white solid; yield: 48 mg, 74.22%; melting range: 212–214°C; ^{1}H NMR (400 MHz, DMSO) δ 10.38 (s, 1H), 9.22 (d, J = 6.5 Hz, 1H), 8.45 (s, 1H), 8.42–8.36 (m, 2H), 8.05 (d, J = 8.2 Hz, 2H), 7.89 (dd, J = 13.9, 8.4 Hz, 4H), 7.62 (s, 1H); ^{13}C NMR (126 MHz, DMSO) δ 158.68 (s), 146.07 (s), 145.44 (s), 139.52 (s), 129.94 (s), 127.51 (s), 126.35 (s), 126.25–125.63 (m), 106.84 (s); UPLC–MS: *m/z* calculated for $C_{22}H_{12}ClF_6N_5$: 495.81; observed mass: 496.8 $[M + H]^+$.

*N-(4-Chloro-5-methoxypyrimidin-2-yl)-3,5-bis(4-(trifluoromethyl)-phenyl)pyrazin-2-amine (**5d**)*

Off-white solid; yield: 58 mg, 84.5%; melting range: 177–179°C; ^{1}H NMR (500 MHz, $CDCl_3$) δ 8.85 (s, 1H), 8.20–8.19 (d, J = 8.0 Hz, 2H), 7.93–7.91 (d, J = 8.0 Hz, 2H), 7.79–7.76 (m, 4H), 7.70–7.68 (d, J = 8.5 Hz, 2H), 3.95 (s, 3H); ^{13}C NMR (126 MHz, $CDCl_3$) δ 150.86 (s), 150.76 (s), 147.22 (s), 145.52 (s), 143.79 (s), 141.19 (s), 140.03 (s), 139.01 (s), 138.43 (s), 136.33 (s), 131.67 (s), 131.52 (s), 131.41 (s), 131.26 (s), 131.00 (s), 130.74 (s), 128.34 (s), 127.83 (s), 126.96 (s), 126.00–125.97 (d), 125.61–125.58 (d), 125.09 (s), 124.98 (s), 122.92 (s), 122.81 (s), 56.52 (s); UPLC–MS: *m/z* calculated for $C_{23}H_{14}ClF_6N_5O$: 525.83; observed mass: 526.2 $[M + H]^+$.

*6-N-{3,5-Bis[4-(trifluoromethyl)phenyl]pyrazin-2-yl}-N-(5-cyanopyridin-2-yl)amino)pyridine-3-carbonitrile (**5e**)*

Off-white solid; yield: 66 mg, 86.12%; melting range: 206–208°C; ^{1}H NMR (500 MHz, $CDCl_3$) δ 8.99 (s, 1H), 8.49–8.48 (t, J = 2.0 Hz, 2H), 8.26–8.25 (d, J = 8.5 Hz, 2H), 7.81–7.78 (m, 6H), 7.54–7.52 (d, J = 8.5 Hz, 2H), 7.13–7.11 (d, J = 8.5 Hz, 2H); ^{13}C NMR (126 MHz, $CDCl_3$) δ 157.20 (s), 152.20 (s), 150.15 (s), 149.88 (s), 148.90 (s), 140.78 (s), 140.35 (s), 139.34 (s), 138.48 (s), 128.53 (s), 127.44 (s), 126.17–126.15 (d), 125.47–125.45 (d), 116.32 (s), 115.97

TABLE 4 ADME properties of synthesized compounds

Ligand	miLogP (−0.4 to 5.9)	TPSA (30–140 Å^2)	MW (<520)	HBA (<10)	HBD (<5)	Rotor (<7)	LogP (<5)	HIA	$CaCO_2$	BBB (−1.2 to +1.2)	Violations
5a	8.84	37.81	613.34	3	1	6	5.34	0.9818	0.6713	0.9690	2
5b	6.34	74.50	485.39	5	1	6	3.79	0.9966	0.6816	0.9524	1
5c	6.70	63.59	494.81	5	1	6	4.19	0.9966	0.7301	0.9725	1
5d	6.88	72.83	525.84	6	1	7	4.14	1.000	0.6286	0.9404	2
5e	6.71	102.39	587.49	7	0	7	4.63	0.9922	0.6978	0.9426	2
6a	7.53	37.81	477.35	3	1	4	3.52	0.9479	0.7461	0.9615	1
6b	4.55	74.50	349.40	5	1	4	1.96	0.9874	0.7790	0.9327	0
6c	4.91	63.59	359.82	5	1	4	2.37	0.9900	0.8078	0.9650	0
6d	5.09	72.83	389.85	6	1	5	2.32	1.0000	0.6812	0.9415	1
6e	4.92	102.39	451.49	7	0	5	2.81	0.9712	0.8053	0.9302	0
7a	8.63	37.81	546.24	3	1	4	5.14	0.9743	0.7510	0.9659	2
7b	5.91	74.50	418.29	5	1	4	3.58	0.9887	0.7738	0.9428	1
7c	6.27	63.59	428.71	5	1	4	3.99	0.9900	0.8078	0.9650	1
7d	6.45	72.83	458.74	6	1	5	3.94	1.0000	0.6812	0.9415	1
7e	6.27	102.39	520.38	7	0	5	4.43	0.9745	0.7710	0.9287	2
8a	8.36	37.81	505.40	3	1	4	3.21	0.9434	0.7324	0.9595	2
8b	5.45	74.50	377.45	5	1	4	1.66	0.9906	0.7650	0.9059	1
8c	5.81	63.59	387.87	5	1	4	2.07	0.9925	0.7872	0.9531	1
8d	5.99	72.83	417.90	6	1	5	2.02	1.0000	0.6826	0.9397	1
8e	5.82	102.39	479.55	7	0	5	2.50	0.9781	0.8033	0.9084	1

Abbreviations: ADME, absorption, distribution, metabolism, excretion; BBB, blood–brain barrier; HBA, hydrogen bond acceptor; HBD, hydrogen bond donor; HIA, human intestinal absorption; MW, molecular weight; Rotor: number of rotatable groups; TPSA, topological polar surface area.

(s), 105.16 (s); UPLC–MS: *m/z* calculated for $C_{30}H_{15}F_6N_7$: 587.48; observed mass: 589.1 $[M+H]^+$.

N-*(4-Iodo-3,5-dimethylphenyl)-3,5-diphenylpyrazin-2-amine (**6a**)*

Off-white solid; yield: 70 mg, 72.5%; melting range: 198–200° C; ^{1}H NMR (500 MHz, $CDCl_3$) δ 8.60 (s, 1H), 7.99–7.98 (d, J = 7.0 Hz, 2H), 7.79–7.78 (d, J = 7.0 Hz, 2H), 7.59–7.56 (t, J = 14.5 Hz, 2H), 7.53–7.50 (t, J = 14.5 Hz, 1H), 7.47–7.44 (t, J = 15.0 Hz, 2H), 7.38–7.35 (t, J = 14.5, 1H), 7.31 (s, 2H), 6.78 (s, 1H), 2.46 (s, 6H); ^{13}C NMR (126 MHz, $CDCl_3$) δ 147.90 (s), 143.06 (s), 142.54 (s), 141.60 (s), 137.11 (s), 136.93 (s), 136.73 (s), 129.49–129.43 (d), 128.83–128.68 (d), 128.33 (s), 125.86 (s), 118.22 (s), 29.74 (s); UPLC–MS: *m/z* calculated for $C_{24}H_{20}IN_3$: 477.34; observed mass: 478 $[M+H]^+$.

*6-(3,5-Diphenylpyrazin-2-ylamino)pyridine-3-carbonitrile (**6b**)*

White solid; yield: 56 mg, 79.27%; melting range: 211–212°C; ^{1}H NMR (400 MHz, DMSO) δ 9.69 (s, 1H), 9.01 (s, 1H), 8.45 (dd, J = 2.3, 0.6 Hz, 1H), 8.17 (d, J = 7.6 Hz, 2H), 8.03 (dd, J = 8.8, 2.3 Hz, 1H), 7.84 (dd, J = 7.9, 1.5 Hz, 2H), 7.56 (dd, J = 17.0, 8.6 Hz, 3H), 7.52–7.44 (m, 4H); ^{13}C NMR (126 MHz, DMSO) δ 152.64 (s), 145.60 (s), 145.43 (s), 141.06 (s), 137.94 (s), 129.76 (s), 129.50 (d), 129.02 (s), 128.82 (s), 126.69 (s), 111.09 (s), 100.04 (s); UPLC–MS: *m/z* calculated for $C_{22}H_{15}N_5$: 349.39; observed mass: 350.5 $[M+H]^+$.

*6-Chloro-*N*-(3,5-diphenylpyrazin-2-yl)pyrimidin-4-amine (**6c**)*

Off-white solid; yield: 52 mg, 71.52%; melting range: 198–200°C; ^{1}H NMR (400 MHz, $CDCl_3$) δ 8.78 (s, 1H), 8.56–8.54 (d, J = 7.0 Hz, 2H), 8.08–8.06 (d, J = 7.24 Hz, 2H), 7.98 (s, 1H), 7.79–7.77 (d, J = 6.88 Hz, 2H), 7.65–7.56 (m, 3H), 7.54–7.50 (t, J = 14.76, 2H), 7.48–7.44 (t, J = 14.44 Hz, 1H); ^{13}C NMR (76 MHz, $CDCl_3$) δ 160.65 (s), 157.94 (s), 156.88 (s), 145.09 (s), 143.92 (s), 135.77–134.50 (t), 129.0–127.70 (m), 125.31 (s), 106.65 (s); UPLC–MS: *m/z* calculated for $C_{20}H_{14}ClN_5$: 359.81; observed mass: 360.4 $[M+H]^+$.

N-*(4-Chloro-5-methoxypyrimidin-2-yl)-3,5-diphenylpyrazin-2-amine (**6d**)*

Off-white solid; yield: 65 mg, 82.51%; melting range: 158–160°C; ^{1}H NMR (400 MHz, DMSO) δ 9.98 (s, 1H), 9.14 (s, 1H), 8.26–8.20 (m, 2H), 7.90 (s, 1H), 7.75 (dd, J = 8.0, 1.4 Hz, 2H), 7.61–7.50 (m, 3H), 7.42–7.34 (m, 3H), 3.89 (s, 3H); ^{13}C NMR (126 MHz, DMSO) δ 153.58 (s), 149.95 (s), 149.26 (s), 148.87 (s), 144.46 (s), 140.61 (s), 138.93 (s), 137.99 (s), 137.39 (s), 135.97 (s), 130.26 (s), 129.52 (s), 129.31 (s),

128.61 (s), 128.37 (s), 127.16 (s), 57.19 (s); UPLC–MS: *m/z* calculated for $C_{21}H_{16}ClN_5O$: 389.84; observed mass: 390.1 $[M + H]^+$.

*6-[*N*-(5-Cyanopyridin-2-yl)-*N*-(3,5-diphenylpyrazin-2-yl)amino]-pyridine-3-carbonitrile (**6e**)*

Off-white solid; yield: 78 mg, 85.62%; melting range: 121–123°C; ^{1}H NMR (500 MHz, $CDCl_3$) δ 8.92 (s, 1H), 8.475–8.471 (d, J = 2.0 Hz, 2H), 8.15–8.13 (d, J = 6.5 Hz, 2H), 7.75–7.73 (dd, J = 2.0 Hz, J = 2.0 Hz, 2H), 7.62–7.60 (t, J = 8.0 Hz, 2H), 7.55–7.51 (m, 3H), 7.26–7.23 (m, 3H), 7.10–7.08 (d, J = 9.0 Hz, 2H); ^{13}C NMR (126 MHz, $CDCl_3$) δ 157.37 (s), 152.03 (s), 151.46 (s), 151.20 (s), 147.74 (s), 140.42 (s), 139.48 (s), 136.02 (s), 135.46 (s), 130.34 (s), 129.57 (s), 129.14 (s), 128.44 (s), 128.05 (s), 127.14 (s), 116.65 (s), 116.11 (s), 104.59 (s). UPLC–MS: *m/z* calculated for $C_{28}H_{17}N_7$: 451.48; observed mass: 452.1 $[M + H]^+$.

*6-[3,5-Bis(4-chlorophenyl)pyrazin-2-ylamino]pyridine-3-carbonitrile (**7b**)*

Off-white solid; yield: 52 mg, 78.62%; melting range: 252–255°C; ^{1}H NMR (500 MHz, $CDCl_3$) δ 8.68 (s, 1H), 8.60–8.58 (dd, J = 0.5 Hz, 1H), 8.49–8.49 (d, J = 1.5 Hz, 1H), 7.97–7.95 (d, J = 8.5 Hz, 2H), 7.93–7.89 (m, 2H), 7.73–7.72 (d, J = 8.5 Hz, 2H), 7.59–7.57 (d, J = 8.5 Hz, 2H), 7.47–7.45 (d, J = 8.5 Hz, 2H); ^{13}C NMR (126 MHz, $CDCl_3$) δ 154.77 (s), 151.89 (s), 145.41 (s), 144.42 (s), 141.67 (s), 141.15 (s), 136.78 (s), 136.35 (s), 135.38 (s), 134.50 (s), 134.01 (s), 130.11 (s), 129.91 (s), 129.23 (s), 127.39 (d), 117.33 (s), 111.77 (s), 102.62 (s); UPLC–MS: *m/z* calculated for $C_{22}H_{13}Cl_2N_5$: 418.28; observed mass: 419.4 $[M + H]^+$.

*N-[3,5-Bis(4-chlorophenyl)pyrazin-2-yl]-6-chloropyrimidin-4-amine (**7c**)*

Off-white solid; yield: 57 mg, 84.04%; melting range: 206–208°C; ^{1}H NMR (400 MHz, $CDCl_3$) δ 8.75 (s, 1H), 8.55–8.51 (d, J = 14.96 Hz, 2H), 8.01–7.98 (t, 2H), 7.87 (s, 1H), 7.73–7.71 (d, J = 8.44 Hz, 2H), 7.61–7.59 (d, J = 8.4 Hz, 2H), 7.50–7.48 (d, J = 8.52 Hz, 2H); ^{13}C NMR (76 MHz, $CDCl_3$) δ 161.81 (s), 158.75 (s), 157.90 (s), 145.00 (s), 141.86 (s), 136.87–136.48 (d), 135.60 (s), 134.31 (s), 133.73 (s), 130.09–129.95 (d), 129.27 (s), 127.49 (s), 107.80 (s). UPLC–MS: *m/z* calculated for $C_{20}H_{12}Cl_3N_5$: 428.7; observed mass: 429.4 $[M + H]^+$.

*N-(4-Chloro-5-methoxypyrimidin-2-yl)-3,5-(4-chlorophenyl)pyrazin-2-amine (**7d**)*

Off-white solid; yield: 51 mg, 70.30%; melting range: 200–203°C; ^{1}H NMR (500 MHz, $CDCl_3$) δ 8.74 (s, 1H), 8.01–7.99 (d, J = 8.0 Hz, 2H), 7.76 (s, 2H), 7.73–7.71 (d, J = 8.5 Hz, 2H), 7.47–7.45 (d, J = 8.0 Hz, 2H), 7.40–7.39 (d, J = 8.5 Hz, 2H), 3.91 (s, 3 H); ^{13}C NMR (126 MHz, $CDCl_3$) δ 151.21 (s), 150.90 (s), 147.56 (s), 145.67 (s), 143.05 (s), 140.04 (s), 137.56 (s), 136.05 (s), 135.93–135.88 (d), 135.40–135.26 (d), 134.22 (s), 129.43 (s), 129.24 (s), 128.93 (s), 127.92 (s), 56.53 (s); UPLC–MS: *m/z* calculated for $C_{21}H_{14}Cl_3N_5O$: 458.73; observed mass: 460.4 $[M + H]^+$.

*6-{N-[3,5-Bis(4-chlorophenyl)pyrazin-2-yl]-N-(5-cyanopyridin-2-yl)amino}pyridine-3-carbonitrile (**7e**)*

Off-white solid; yield: 70 mg, 85.06%; melting range: 145–147°C; ^{1}H NMR (500 MHz, $CDCl_3$) δ 8.89 (s, 1H), 8.49–8.48 (d, J = 2.0 Hz, 2H), 8.08–8.07 (d, J = 8.5 Hz, 2H), 7.79–7.77 (dd, J = 2.0 Hz, J = 2.0 Hz, 2H), 7.63–7.61 (d, J = 8.5 Hz, 2H), 7.52–7.50 (d, J = 8.5 Hz, 2H), 7.23–7.22 (d, J = 8.5 Hz, 2H), 7.12–7.10 (d, J = 8.5 Hz, 2H); ^{13}C NMR (126 MHz, $CDCl_3$) δ 157.23 (s), 152.13 (s), 150.25–150.17 (d), 147.89 (s), 140.66 (s), 139.46 (s), 136.81 (s), 136.02 (s), 134.27 (s), 133.72 (s), 129.45–129.38 (d), 128.80 (s), 128.35 (s), 116.49 (s), 115.91 (s), 104.91 (s); UPLC–MS: *m/z* calculated for $C_{28}H_{15}Cl_2N_7$: 520.37; observed mass: 521.4 $[M + H]^+$.

*N-(4-Iodo-3,5-dimethylphenyl)-3,5-di-*p*-tolylpyrazin-2-amine (**8a**)*

Off-white solid; yield: 65 mg, 70.82%; melting range: 202–204°C; ^{1}H NMR (500 MHz, $CDCl_3$) δ 8.54 (s, 1 H), 7.88–7.87 (d, J = 7.5 Hz, 2H), 7.67–7.66 (d, J = 7.5 Hz, 2H), 7.37–7.36 (d, J = 7.5 Hz, 2H), 7.31 (s, 2 H), 7.26–7.24 (d, J = 7.0 Hz, 2H), 6.78 (s, 1H), 2.45 (s, 9H), 2.39 (s, 3H); ^{13}C NMR (126 MHz, $CDCl_3$) δ 147.65 (s), 143.13 (s), 142.48 (s), 141.66 (s), 139.52 (s), 139.32 (s), 138.20 (s), 136.53 (s), 134.23 (s), 133.89 (s), 130.07 (d), 129.52 (s), 128.57 (s), 125.74 (s), 118.03 (s), 99.43 (s), 29.74 (s), 21.42–21.27 (d); UPLC–MS: *m/z* calculated for $C_{26}H_{24}IN_3$: 506.39; observed mass: 507.2 $[M + H]^+$.

*6-(3,5-Di-*p*-tolylpyrazin-2-ylamino)pyridine-3-carbonitrile (**8b**)*

Off-white solid; yield: 56 mg, 81.71%; melting range: 218–220°C; ^{1}H NMR (400 MHz, $CDCl_3$) δ 8.67–8.61 (t, 2H), 8.47–8.44 (d, J = 1.52 Hz, 1H), 8.25 (s, 1H), 7.96–7.91 (m, 3H), 7.69–7.67 (d, J = 7.96 Hz, 2H), 7.43–7.41 (d, J = 7.84 Hz, 2H), 7.32–7.28 (t, 2H), 2.48–2.44 (d, J = 18.56, 6H); ^{13}C NMR (76 MHz, $CDCl_3$) δ 154.91 (s), 151.31 (s), 145.83 (s), 144.82 (s), 143.10 (s), 141.18 (s), 140.10 (s), 139.19 (s), 136.08 (s), 133.48 (s), 132.84 (s), 130.24 (s), 129.67 (s), 128.66 (s), 126.12 (s), 117.34 (s), 111.77 (s), 101.93 (s), 21.42–21.32 (d); UPLC–MS: *m/z* calculated for $C_{24}H_{19}N_5$: 377.44; observed mass: 378.9 $[M + H]^+$.

*6-Chloro-*N*-(3,5-di-*p*-tolylpyrazin-2-yl)pyrimidin-4-amine (**8c**)*

Off-white solid; yield: 55 mg, 80.09%; melting range: 192–195°C; ^{1}H NMR (400 MHz, $CDCl_3$) δ 8.72 (s, 1H), 8.539–8.530 (d, J = 3.68 Hz, 2H), 8.17 (s, 1H), 7.97–7.95 (d, J = 8.12 Hz, 2H), 7.67–7.65 (d, J = 8.0 Hz, 2H), 7.43–7.41 (d, J = 7.84 Hz, 2H), 7.33–7.28 (t, 2H), 2.48–2.44 (d, J = 19.4, 6H); ^{13}C NMR (76 MHz, $CDCl_3$) δ 161.61 (s), 158.68 (s), 157.17 (s), 146.49 (s), 144.33 (s), 143.38 (s), 140.25 (s), 139.44 (s), 136.22 (s), 133.28 (s), 132.53 (s), 130.29 (s), 129.71 (s), 128.97 (s), 128.64 (s), 126.24 (s), 107.62 (s), 21.41–21.33 (d); UPLC–MS: *m/z* calculated for $C_{22}H_{18}ClN_5$: 387.86; observed mass: 389.2 $[M + H]^+$.

*N-(4-Chloro-5-methoxypyrimidin-2yl)-3,5-di-*p*-tolylpyrazin-2-amine (**8d**)*

Off-white solid; yield: 60 mg, 75.66%; melting range: 211–213°C; ^{1}H NMR (400 MHz, $CDCl_3$) δ 8.78 (s, 1H), 7.99 (s, 2H), 7.83–7.78 (d, J = 20 Hz, 2H), 7.69 (s, 2H), 7.30–7.28 (d, J = 6.4 Hz, 4H), 3.90 (s, 3H), 2.42 (s, 6H); ^{13}C NMR (100 MHz, $CDCl_3$) δ 170.81 (s), 151.69–151.20 (d), 148.50 (s), 146.13 (s), 142.76 (s), 140.12 (s), 139.64–139.44 (d), 137.31 (s), 135.83 (s), 134.17 (s), 133.32 (s), 129.69–129.49 (d), 128.24 (s), 126.58 (s), 56.50 (s), 21.55–21.39 (d); UPLC–MS: *m/z* calculated for $C_{23}H_{20}ClN_5O$: 417.89; observed mass: 418.3 $[M + H]^+$.

*6-[N-(5-Cyanopyridin-2-yl)-N-(3,5-di-p-tolylpyrazin-2-yl)amino]-pyridine-3-carbonitrile (**8e**)*

Off-white solid; yield: 74 mg, 86.13%; melting range: 201–203°C, ^{1}H NMR (400 MHz, $CDCl_3$) δ 8.89 (s, 1H), 8.49 (s, 2H), 8.06 (d, 2H), 7.76 (s, 2H), 7.55 (s, 2H), 7.35 (s, 2H), 7.12–7.05 (d, J = 27.6 Hz, 4H), 2.46 (s, 3H), 2.30 (s, 3H); ^{13}C NMR (100 MHz, $CDCl_3$) δ 157.38 (s), 151.99–151.50 (d), 151.14 (s), 147.11 (s), 140.64–140.40 (s), 139.74 (s), 138.99 (s), 133.13–132.73 (d), 129.87 (s), 129.17 (s), 127.03 (s), 116.79 (s), 116.05 (s), 116.05 (s), 104.43 (s), 21.47–21.32 (d); UPLC–MS: *m/z* calculated for $C_{30}H_{21}N_7$: 479.53; observed mass: 480.3 $[M + H]^+$.

4.2 | Biological assays

4.2.1 | Experimental procedure for antituberculosis studies

LJ medium was used to detect the anti-TB activity of synthesized 2-aryl-3,5-disubstituted pyrazine derivatives. Plain LJ medium was prepared as per the standard guidelines of culture and the DST of Mtb (RNTCP standard SOPs maintained by the DST-accrediting laboratories throughout the country) at NTI, Bangalore, India. For the 5 mg of each PZA derivative weighed accurately and dissolved in 5 ml of dimethylformamide solvent. To test the MIC, three different drug concentrations (15, 25, and 50 µg/ml) were prepared using the parent stock solution. McCarteny bottles (imported unbreakable with sealed caps) were used to load the medium, and in each bottle 5 ml of prepared drug with LJ medium is dispersed in a laminar wood. All the bottles containing the drug medium were inspissated at 85°C until the liquid form of the medium solidified as slants, which were further QC tested by keeping the LJ slants under 37°C incubation for 24 hr. For all the tested Mtb strains, including standard H37Rv, Mtb strain 1, and Mtb strain 2, inoculum were prepared separately and inoculated in the drug-containing medium along with positive controls (RMP and INH) used for this study. All cultures were examined 48 hr after inoculation at 37°C in a walk-in incubator to detect cross-contamination. Thereafter, cultures were examined weekly, up to 8 weeks (to be declared as sensitive), on a specified day of the week. Culture results were taken manually based on the typical morphological characteristics of Mtb.

4.2.2 | Experimental procedure for cytotoxicity determination

Cytotoxicities of the synthesized 2-aryl-3,5-disubstituted pyrazine derivatives were tested in human embryonic kidney cells (HEK-293) using the MTT assay method. HEK-293 cells were cultured in Dulbecco's modified Eagle's medium supplemented with 10% fetal bovine serum, 10,000 units/ml penicillin, 10 mg/ml streptomycin, and 25 mg/ml amphotericin B in a 96-well plate (~15×10^3 cells/well). After 24 hr, the medium was removed and replaced with varying concentrations of pyrazine derivatives for another 24 hr. All compounds were dissolved in DMSO and diluted with fresh medium. The final DMSO concentration was 1.5%. Nearly 24 hr after the addition of compounds, the MTT assay was carried out by treating the cells with 5 mg/ml MTT solution in phosphate-buffered solution. After 3 hr of MTT treatment, the formazan crystals formed were dissolved in 100 ml DMSO. The absorbance was measured at 540 nm using a PerkinElmer EnSpire Multimode Plate Reader. Cell viability was expressed as the percentage of viable cells compared with untreated DMSO control cells.

4.2.3 | Protein structure prediction

The catalytic domain of protein kinase (PknB) from the Mtb protein sequence was retrieved from the UniProt database (UID: P9WI81). The selected protein sequences were used to predict sequence similarity and to predict sequence templates by PSI-BLAST.[24] The selected template sequences were used to build three-dimensional protein structures using SWISS-MODEL.[25] Homology modeling by Swiss PDB Viewer helps to predict the complexity of the protein structures which was validated to check overall protein quality, and stereochemical activities of atoms and amino acids were predicted by structural analysis and verification server (SAVES).[26] The conformational complexity of protein structures was used to predict the active site of amino acids that helps in ligand binding and evaluated using CastP calculation server. The best complex protein structures were used for molecular docking.

The synthetic chemical compounds were listed based on molecular weight and the resultant compounds were used as the training set. To design the chemical structures, ACD/ChemSketch software[27] was used to add all chemical compositions and the final output was saved in MOL2 format. The training sets were used to predict pharmacophore using Molinspiration server[28] and QSAR (quantitative structure–activity relationship) properties were predicted using HyperChem. A training set helps to predict the complex polarity and flexibility, to examine MM3 force fields, to examine HOMO (highest occupied molecular orbital) and LUMO (lowest occupied molecular orbital), and to understand new molecular orbitals in individual compounds.[29] The lead compounds or scaffolds were identified from the diversified compound pool and then subjected to accelerated screening; a screened pool is focused for bio-targets to inhibit diseases. Here, we used structural screening, fragment analysis, and pharmacological analyses to screen the compounds based on the interaction with target apoptotic proteins.

ORCID

Eeda Koti Reddy http://orcid.org/0000-0003-4048-7178

REFERENCES

[1] WHO, Global Tuberculosis Report, **2017**. http://www.who.int/tb/publications/global_report/en/
[2] World Health Organization, **2010**. http://www.who.int/tb/publications/globalreport/2010/en/index.html
[3] C. Lienhardt, P. Glaziou, M. Uplekar, K. Lonnroth, H. Getahun, M. Raviglione, *Nat. Rev. Microbiol.* **2012**, *10*, 407.

[4] G. Craig, A. Daftary, N. Engel, S. O'Driscoll, A. Ioannaki, *Int. J. Infect. Dis.* **2017**, *56*, 90.
[5] S. S. Gautam, R. F. Toole, *J. Pulm. Respir. Med.* **2016**, *6*, 2.
[6] A. I. Zumla, S. H. Gillespie, M. Hoelscher, P. P. Philips, S. T. Cole, I. Abubakar, T. D. McHugh, M. Schito, M. Maeurer, A. J. Nunn, *Lancet Infect. Dis.* **2014**, *14*, 327.
[7] M. Pai, M. A. Behr, D. Dowdy, K. Dheda, M. Divangahi, C. C. Boehme, A. Ginsberg, S. Swaminathan, M. Spigelman, H. Getahun, D. Menzies, M. Raviglione, *Nat. Rev. Dis. Primers* **2016**, *2*, 16076.
[8] J. D. Hosford, M. E. von Fricken, M. Lauzardo, M. Changd, Y. Dai, J. A. Lyon, J. Shuster, K. Fennelly, *Tuberculosis* **2015**, *95*, 112.
[9] P. S. Charifson, A. L. Grillot, T. H. Grossman, J. D. Parsons, M. Badia, S. Bellon, D. D. Deininger, J. E. Drumm, C. H. Gross, A. LeTiran, Y. Liao, N. Mani, D. P. Nicolau, E. Perola, S. Ronkin, D. Shannon, L. L. Swenson, Q. Tang, P. R. Tessier, S. K. Tian, M. Trudeau, T. Wang, Y. Wei, H. Zhang, D. Stamos, *J. Med. Chem.* **2008**, *51*, 5243.
[10] P. S. Shirude, P. Madhavapeddi, J. A. Tucker, K. Murugan, V. Patil, H. Basavarajappa, A. V. Raichurkar, V. Humnabadkar, S. Hussein, S. Sharma, V. K. Ramya, C. B. Narayan, T. S. Balganesh, V. K. Sambandamurthy, *ACS Chem. Biol.* **2013**, *8*, 519.
[11] T. J. Miles, A. J. Hennessy, B. Bax, G. Brooks, B. S. Brown, P. Brown, N. Cailleau, D. Chen, S. Dabbs, T. D. Davies, J. M. Esken, L. Giordano, J. L. Hoover, J. Huang, G. E. Jones, S. K. K. Sukmar, C. Spitzfaden, R. E. Markwell, E. A. Mlingthorn, S. Rittenhouse, M. N. Gwynn, N. D. Pearson, *Bioorg. Med. Chem. Lett.* **2013**, *23*, 5437.
[12] V. Makarov, B. Lechartier, M. Zhang, J. Neres, A. M. van der Sar, S. A. Raadsen, R. C. Hartkoorn, O. B. Ryabova, A. Vocat, L. A. Decosterd, N. Widmer, T. Buclin, W. Bitter, K. Andries, F. Pojer, P. J. Dyson, S. T. Cole, *Mol. Med.* **2014**, *6*, 372.
[13] P. S. Shirude, R. Shandil, C. Sadler, M. Naik, V. Hosagrahara, S. Hameed, V. Shinde, C. Bathula, V. Humnabadkar, N. Kumar, J. Reddy, V. Panduga, S. Sharma, A. Ambady, N. Hegde, J. Whiteaker, R. E. McLaughlin, H. Gardner, P. Madhavapeddi, V. Ramachandran, P. Kaur, A. Narayan, S. Guptha, D. Awasthy, C. Narayan, J. Mahadevaswamy, K. G. Vishwas, V. Ahuja, A. Srivastava, K. R. Prabhakar, S. Bharath, R. Kale, M. Ramaiah, N. R. Choudhury, V. Sambandamurthy, S. M. Solapure, P. S. Iyer, S. Narayanan, M. Chatterji, *J. Med. Chem.* **2013**, *56*, 9701.
[14] J. C. Peter, S. S. Hamish, S. T. T. Amy, B. Adrian, G. F. Scott, B. C. Christopher, U. L. Manisha, M. U. Anna, G. Jerome, M. Magali, Q. Laurence, *Bioorg. Med. Chem. Lett.* **2017**, *27*, 5190–5196.
[15] (a) G. N. Reddy, A. Ranganatham, E. K. Reddy, H. D. Surendra, A. M. Sajith, Y. Shivaraj, K. B. Chandrasekhare, *J. Heterocycl. Chem.* **2019**, *56*, 1117; (b) T. N. Prasad, E. K. Reddy, G. V. Babu, S. F. Basha, S. Anwar, *Synth. Commun.* **2019**, *49*, 1277.
[16] (a) K. Stoffels, V. Mathys, M. Fauville-Dufaux, R. Wintjens, P. Bifani, *Antimicrob. Agents Chemother.* **2012**, *56*, 5186; (b) B. J. Benjamin, A. Aboelela, E. Minaei, E. Longguang, X. Jiang, Z. Xu, U. Ali, K. Fildes, C. Y. Cheung, M. Simon, M. Cook, D. C. Johnson, *J. Med. Chem.* **2018**, *61*, 8299.
[17] J. D. Osborne, T. P. Matthews, T. A. McHardy, N. Proisy, K.-M. J. Cheung, M. Lainchbury, N. Brown, M. I. Walton, P. D. Eve, K. Boxall, J. Katherine, *J. Med. Chem.* **2016**, *59*, 5221.
[18] R. Rahmani, K. Ban, A. J. Jones, L. Ferrins, D. Ganame, M. L. Sykes, V. M. Avery, K. L. White, E. Ryan, M. Kaiser, *J. Med. Chem.* **2015**, *58*, 6753.
[19] Y. Younis, F. Douelle, D. G. Cabrera, C. L. Manach, A. T. Nchinda, T. Paquet, L. J. Street, K. L. White, M. K. Zabiulla, J. T. Joseph, *J. Med. Chem.* **2013**, *56*, 8860.
[20] S. Berg, M. Bergh, S. Hellberg, K. Hoegdin, Y. L. Alfredsson, P. Soederman, S. von Berg, T. Weigelt, M. Ormoe, Y. Xue, *J. Med. Chem.* **2012**, *55*, 9107.
[21] J. Humphrey, N. Kablaoui, S. Kazmirski, M. Kraus, S. Kupchinsky, J. L. John, L. Lingardo, M. A. Marx, D. Richter, S. P. Tanis, *J. Med. Chem.* **2011**, *54*, 8490.
[22] (a) E. K. Reddy, R. Chandran, A. M. Sajith, K. V. Dileep, C. Sadasivan, S. Anwar, *RSC Adv.* **2016**, *6*, 77431; (b) E. K. Reddy, R. Chandran, K. Mantosh, A. M. Sajith, R. V. Omkumar, C. Sadasivan, S. Anwar, *Eur. J. Med. Chem.* **2017**, *139*, 367; (c) B. Savitha, E. K. Reddy, C. S. Ananda Kumar, R. P. Karuvalam, M. S. AliPadusha, V. A. Bakulev, K. H. Narasimhamurthy, A. M. Sajith, M. NibinJoy, *Tetrahedron Lett.* **2019**, *52*, 151332.
[23] G. N. Reddy, E. K. Reddy, A. M. Sajith, Y. Shivaraj, K. B. Chandrashekar, *ChemistrySelect* **2017**, *2*, 7706.
[24] M. K. Hasballah, A. Azhar, N. Rahmi, *Int. J. Trop. Vet. Biomed. Res.* **2016**, *1*, 45.
[25] T. P. Sathishkumar, P. Navaneethakrishnan, S. Hankar, R. Rajasekar, *J. Reinf. Plast. Compos.* **2013**, *32*, 19.
[26] T. Choedon, G. Mathan, V. K. Choedon, *BMC Complement. Altern. Med.* **2015**, *15*, 182.
[27] J. Bethuyne, S. D. Gieter, O. Zwaenepoel, A. Garcia-Pino, K. Durinck, A. Verhelle, G. H. Ghassabeh, F. Speleman, R. Loris, J. Gettemans, *Nucleic Acids Res.* **2014**, *42*, 12928.
[28] Z. Liyuan, G. Lingkun, R. Patricia, S. Stanley, J. R. Paul, J. Shen, Q. Zhang, **2015**.
[29] M. L. Tress, F. Abascal, A. Valencia, *Trends Biochem. Sci.* **2017**, *42*, 98.

SUPPORTING INFORMATION

Additional supporting information may be found online in the Supporting Information section.

How to cite this article: Gangarapu NR, Ranganatham A, Reddy EK, Yellappa S, Chandrasekhar KB. 2-Aminoaryl-3, 5-diaryl pyrazines: Synthesis, biological evaluation against *Mycobacterium tuberculosis* and docking studies. *Arch Pharm.* 2020;e1900368. https://doi.org/10.1002/ardp.201900368